Volume 55(9): 899–909, 2007
Journal of Histochemistry & Cytochemistry
http://www.jhc.org

ARTICLE

# Loss of Caveolin-1 in Bronchiolization in Lung Fibrosis

Nao Odajima, Tomoko Betsuyaku, Yasuyuki Nasuhara, and Masaharu Nishimura

First Department of Medicine, Hokkaido University School of Medicine, Sapporo, Japan

SUMMARY Bronchiolization is a key process in fibrosing lung in which the proliferative status of bronchiolar epithelium changes, leading to abnormal epithelial morphology. Within the context that caveolin-1 acts to suppress epithelial proliferation, we postulated that stimulating epithelial injury would lead to caveolin-1 downregulation and encourage proliferation. The present study evaluates the expression of caveolin-1, especially in bronchiolization, in C57BL/6J mice with bleomycin-induced lung fibrosis and in various types of re-epithelialization in human interstitial pneumonias (IPs). Immunohistochemically, levels of caveolin-1 decreased in the bronchiolar epithelium of mice treated with bleomycin. Levels of caveolin-1 mRNA in the whole lung were decreased at 7 and 14 days. Caveolin-1 mRNA was also decreased in laser-capture microdissection- retrieved bronchiolar epithelial cells at 7 days. Among patients with 12 IPs, including four usual IPs (UIPs) and eight nonspecific IPs (NSIPs), whole lung caveolin-1 was significantly decreased compared with 12 controls at both mRNA and protein levels. By scoring immunointensity, caveolin-1 was significantly reduced in bronchiolization and squamous metaplasia as well as in bronchiolar epithelium in 23 IPs (12 UIPs and 11 NSIPs) compared with bronchiolar epithelium from seven controls. These data suggested that loss of caveolin-1 is associated with abnormal re-epithelialization in lung fibrosis. (J Histochem Cytochem 55:899–909, 2007)

KEY WORDS
caveolin-1
bleomycin
lung fibrosis
bronchiolization
laser-capture microdissection

EPITHELIAL REPAIR after injury is an important step in normal wound-healing processes (Fukuda et al. 1985; Selman et al. 2001). Although excessive re-epithelialization is characteristic of various fibrotic lung disorders (Nettesheim and Szakal 1972; Fukuda et al. 1985; Betsuyaku et al. 2000,2003a), the pathophysiology of abnormal proliferation of bronchiolar epithelial cells such as bronchiolization and squamous metaplasia remains obscure.

Caveolae are 50- to 100-nm vesicular invaginations of the cell surface plasma membrane that are thought to arise due to the local accumulation of cholesterol, glycosphingolipids, and the 21- to 24-kDa integral membrane protein caveolin-1, which is a principal component of caveolar membranes and plays physiological roles in intracellular vesicular transport such as transcytosis and endocytosis and signal transduction (Liu et al. 2002; Cohen et al. 2004). In normal adult lungs, caveolin-1 is preferentially located in endothelial cells, type I epithelial cells, smooth muscle cells, and fibroblasts (Cohen et al. 2004) and is detectable in bronchiolar epithelial cells (Kasper et al. 1998; Kato et al. 2004). Targeted caveolin-1 disruption results in profound disruption of the vascular system and thickening of alveolar septa and fibrosis in the lung, accompanied by marked hypertrophy of type II epithelial cells in mice (Drab et al. 2001). Caveolin-1 is indeed downregulated in alveolar epithelium in experimental irradiation-induced lung injury (Kasper et al. 1998) and in bleomycin-induced lung fibrosis (Barth et al. 2006), implying that the loss of alveolar caveolin-1 could be an early indicator of serious type I epithelial cell injury in the process of fibrogenesis. Analysis of global gene expression using microarrays has recently revealed that caveolin-1 is downregulated in whole lung tissue of patients with idiopathic pulmonary fibrosis (IPF) (Wang et al. 2006). On the other hand, caveolin-1 overexpression prevents cell transformation (Engelman et al. 1997; Galbiati et al. 1998) and promotes cell-cycle arrest and senescence (Galbiati et al. 2001; Volonte et al. 2002), suggesting that caveolin-1 could suppress the

Correspondence to: Tomoko Betsuyaku, MD, PhD, First Department of Medicine, Hokkaido University School of Medicine, N-15, W-7, Kita-ku, Sapporo 060-8638, Japan. E-mail: bytomoko@med.hokudai.ac.jp

Received for publication February 1, 2007; accepted April 9, 2007 [DOI: 10.1369/jhc.7A7203.2007].



0022-1554/07/$3.30

proliferation and migration of cancer cells. The reduced expression of caveolin-1 in various human cancer cells such as breast, lung, colorectal, and ovary, as well as in sarcomas, supports this notion (Williams and Lisanti 2005; Torres et al. 2006). We thus speculated that caveolin-1 is specifically downregulated in abnormal re-epithelialization and is associated with the proliferative phenotype in lung fibrosis. For more than two decades, bleomycin-induced lung injury in experimental animals has been used as a model to investigate the cell biology and histopathology of pulmonary lesions that resemble human IPF (Thrall and Scalise 1995). Studies of this model have helped uncover the complexity of mechanisms involved in human disease. Although bleomycin may damage structural cells of the lungs directly (Simon and Paine 1995; Sato et al. 1999), its principal mode of action in leading to IPF-like pathology seems to be via endogenous mediators of inflammation, fibrinolysis, and proliferation. Here we assessed caveolin-1 expression from the perspective of bronchiolization in mouse bleomycin-induced lung fibrosis and in various types of abnormal re-epithelialization in human IPs.

## Materials and Methods

### Animals and Experimental Protocols

Male C57BL/6J mice (6–8 weeks old) were housed in plastic chambers with free access to food and water in a pathogen-free animal facility. After an IP injection of ketamine and xylazine for sedation and anesthesia, 0.05 U of bleomycin (Blenoxane; Nippon Kayaku, Tokyo, Japan) was intratracheally administered as described (Betsuyaku et al. 2000). After 7 and 14 days, the animals were killed, and their lungs were processed as described below. Mice that had not undergone manipulation served as controls. The Ethical Committee on Animal Research of Hokkaido University School of Medicine approved all experimental protocols and procedures associated with the study.

### Tissue Processing of Mouse Lungs

Immediately after the animals were killed, the thorax was opened, and whole lungs were perfused with saline through the right ventricle to remove blood. The lungs were fixed by inflation with 10% buffered formalin for 24 hr and embedded in paraffin for immunohistochemistry ($n$=2–3 per time point) or inflated with diluted Tissue-Tek OCT (Sakura Finetek; Torrance, CA) and then stored frozen at −80C for RNA and protein extraction as described ($n$=5 per time point) (Betsuyaku et al. 2001).

### Patients and Tissue Collection

The study population was comprised of 23 patients with IP, including 12 with usual interstitial pneumonia (UIP) and 11 with nonspecific interstitial pneumonia (NSIP). Patients with UIP were 65 ± 1 year old, female/male ratio was 6/6, and nine patients were smokers, whereas patients with NSIP were 59 ± 4 years, female/male ratio was 8/3, and two patients were smokers. Applying the diagnostic criteria of the American Thoracic Society/European Respiratory Society (ATS/ERS 2002) international multidisciplinary consensus classification, each diagnosis was based on the standard clinical criteria and histopathological analyses of lung tissues obtained by video-assisted thoracoscopy-guided lung biopsy or surgical lobectomy, as previously described (Odajima et al. 2006). All control lung specimens were obtained from 17 patients who had never smoked (3 males and 14 females, aged 64 ± 2 years) and who underwent lung lobectomy for small peripheral tumors. Immediately after biopsy or lobar resection, tissues were inflated with diluted Tissue-Tek OCT (Sakura Finetek) as described above, frozen as soon as possible, and stored at −80C before RNA and protein extraction (IPs, $n$=12 with 4 UIPs and 8 NSIPs among 23 IPs; controls, $n$=12) or were fixed by manual inflation with 10% neutral-buffered formalin using a 23-gauge needle and embedded in paraffin for immunohistochemistry (IPs, $n$=23 with 12 UIPs and 11 NSIPs; controls, $n$=7), in which only two control lungs were overlapped for both studies.

Written informed consent was obtained from all patients, and the Ethics Committee of Hokkaido University School of Medicine approved the study. Vital capacity (VC), forced expiratory volume in 1 sec (FEV1), and diffusing capacity for carbon monoxide ($DL_{CO}$) were measured in all patients (CHESTAC-55V; Chest Co., Tokyo, Japan) before surgery. All patients also underwent high-resolution computed tomography scans, arterial blood gas analysis, and serum Krebs von den Lungen-6 (KL-6) measurements (Yokoyama et al. 1998).

### Immunohistochemistry

Caveolin-1 immunohistochemistry proceeded as described (Betsuyaku et al. 2003b) using a CSA kit (Dako Japan; Kyoto, Japan) according to the manufacturer's protocol. Tissue sections were incubated with a rabbit anti-caveolin-1 antibody (N20 sc894; Santa Cruz Biotechnology, Santa Cruz, CA) diluted 1:1000 for mice and 1:2000 for humans overnight at 4C. Sections were counterstained with hematoxylin. Staining of endothelial cells and lymphocytes served as internal positive and negative controls, respectively, for caveolin-1. Sections were stained for Ki-67 with a mouse anti-Ki-67 antibody (clone MIB-1; Dako Japan) and 0.1 mM EDTA buffer (pH 8.0) for antigen retrieval in an automated immunostainer (Ventana NX; Ventana Japan, Yokohama, Japan).

### Semiquantitative Immunohistochemistry for Caveolin-1 in Human Lungs

Because the amount and distribution of abnormal epithelial cells within the lungs was heterogeneous, immunostained tissue sections from one block per patient were thoroughly investigated to identify more than one group of each cell type. Staining intensity of caveolin-1 expression was then scored for each cell type at the same magnification using a visual scoring method with grades ranging from 0 to 3 (0, no staining; 1, moderate staining; 2, intense staining; 3, very intense staining), as described (de Boer et al. 2000; Odajima et al. 2006). Intensity was scored twice in a blinded manner, in which the observer (NO) was unaware of any clinical details of the patients. Based on significant Spearman's rank correlation coef-

ficients between two observations for caveolin-1 ($p<0.0001$), only the latter data set is presented.

### Laser-Capture Microdissection (LCM) of Bronchiolar Epithelial Cells in Mouse Lung

Bronchiolar epithelial cells were selectively harvested from the lungs by LCM using a PixCell II System (Arcturus Engineering; Mountain View, CA) as described (Betsuyaku et al. 2001). After the samples were captured on transfer films (CapSure Macro LCM Caps, LCM0211; Arcturus Engineering), nonspecific attached components were removed using adhesive tape (CapSure Cleanup Pad, LCM0206; Arcturus Engineering). Bronchiolar epithelial cells were retrieved from the junction of the terminal bronchioles and alveolar ducts and proximally along airways of up to ~250 μm in diameter, as described (Betsuyaku and Senior 2004). At least six bronchioles were randomly selected, and cells were collected from each mouse specimen using a total of 5000 laser bursts. We analyzed mRNA in non-stained serial sections (whole lung tissue specimens) adjacent to the sections examined by LCM.

### Quantitative Reverse Transcriptase–Polymerase Chain Reaction

Total RNA was extracted using the RNeasy Mini Kit (Qiagen; Hilden, Germany). cDNA templates were synthesized using reverse transcriptase (RT) (Applied Biosystems; Foster City, CA), and mRNA levels were quantified by the 5′-exonuclease-based fluorogenic polymerase chain reaction (PCR) using a 7300 Real Time PCR System (Applied Biosystems) as described (Betsuyaku et al. 2001, Betsuyaku and Senior 2004), with TAKARA master mix (TAKARA BIO INC.; Shiga, Japan) according to the manufacturer's instructions. The relative amount of target mRNA in the samples was assessed by interpolating threshold cycles from a standard curve. TaqMan Gene Expression Assays probes were Hs00184697_m1 for human caveolin-1 and Mm00483057_m1 for murine caveolin-1 (Applied Biosystems), and the levels were normalized against glyceraldehyde-3-phosphatase-dehydrogenase mRNA (human) and β2-microglobulin mRNA (mouse).

### Western Blotting

Frozen lung tissues were homogenized in lysis buffer (T-PER Tissue Protein Extraction Reagent; Pierce Biotechnology, Rockford, IL) containing the protease inhibitors phenylmethylsulfonyl fluoride (100 mM), antipain (1.2 mg/ml), aprotinin (2 mg/ml), pepstatin A (0.5 mg/ml), and leupeptin (1 mg/ml). After the samples were centrifuged at 10,000 × g for 5 min at 4C, the total protein concentration of the supernatant was determined using the BCA method (Pierce Biotechnology). Mouse and human samples (15 and 10 μg of protein, respectively) were resolved by electrophoresis under reducing conditions as described (Betsuyaku et al. 2003a). Transferred membranes were incubated overnight at 4C with rabbit anti-caveolin-1 antibody (N20 sc-894) diluted 1:2000 followed by horseradish peroxidase-conjugated anti-rabbit immunoglobulin (Dako Japan) diluted 1:20,000. Membranes were treated with the Immobilon Western Chemiluminescent HRP Substrate (Millipore Corporation; Billerica, MA) and then specific antibody binding was visualized by exposure to photographic film. Because the use of β-actin as a normalizing control is limited in human lung diseases (Glare et al. 2002), loading homogeneity was determined based on an equal amount of total protein in each sample. Immunoreactive signals were analyzed using an Epson 2000 Scanner (Nagano, Japan) and calculated using Scion Image software (Scion Corporation; Frederick, MD).

### Statistical Analysis

Results are expressed as means ± SEM. Data were statistically analyzed using the single factor ANOVA, and Student's unpaired *t*-test was applied to comparisons between groups. Two groups of immunohistochemical results were compared using the Mann-Whitney U test, and differences in the immunointensity of different epithelial cell types between IPs were analyzed using the Kruskal–Wallis test. Spearman's rank correlation coefficients were calculated to assess test–retest reliability (StatView J 5.0; SAS Institute Inc., Cary, NC); $p<0.05$ was considered statistically significant.

## Results

### Localization of Caveolin-1 in Normal and Fibrotic Lungs in Mice

We immunohistochemically localized caveolin-1 in normal and fibrotic mouse lungs. Caveolin-1 was ubiquitously expressed in type I cells and endothelial cells in the normal lungs (Figure 1A) and remained in those cells in alveolar walls even in the damaged lungs induced by bleomycin (Figures 1B–1F). Caveolin-1 was also detected at the apical side of some bronchiolar epithelial cells (Figure 1A), whereas bronchiolar caveolin-1 was barely detected in these cells at 7 days after bleomycin treatment (Figure 1B). At 14 days, caveolin-1 was negative in bronchiolar epithelial cells and in bronchiolization within fibrotic areas (Figures 1C and 1D). Alveolar bronchiolization was identified as cells resembling bronchiolar epithelium lining normal or thickened alveolar walls, often in an acinar formation, as previously described (Betsuyaku et al. 2000). Caveolin-1 was also barely detected in fibroblastic foci (Figures 1E and 1F).

### Caveolin-1 mRNA and Protein in Fibrotic Lung in Mice

Whole lung caveolin-1 mRNA expression was significantly decreased in mice at 7 and 14 days after intratracheal bleomycin administration compared with controls (0.6 ± 0.1 and 0.7 ± 0.1, respectively, vs 1.5 ± 0.1, $p<0.01$) (Figure 2A). Figure 2B shows a representative Western blot of caveolin-1 protein at 22 kDa in whole lung homogenates. Although caveolin-1 protein levels were decreased after bleomycin treatment, differences did not reach statistical significance at 7 days and 14 days after bleomycin treatment compared with untreated controls (3.0 ± 1.5 AU vs 7.8 ± 2.0, $p=0.05$; 3.8 ± 1.3 vs 7.8 ± 2.0, NS, respectively) (Figure 2C).

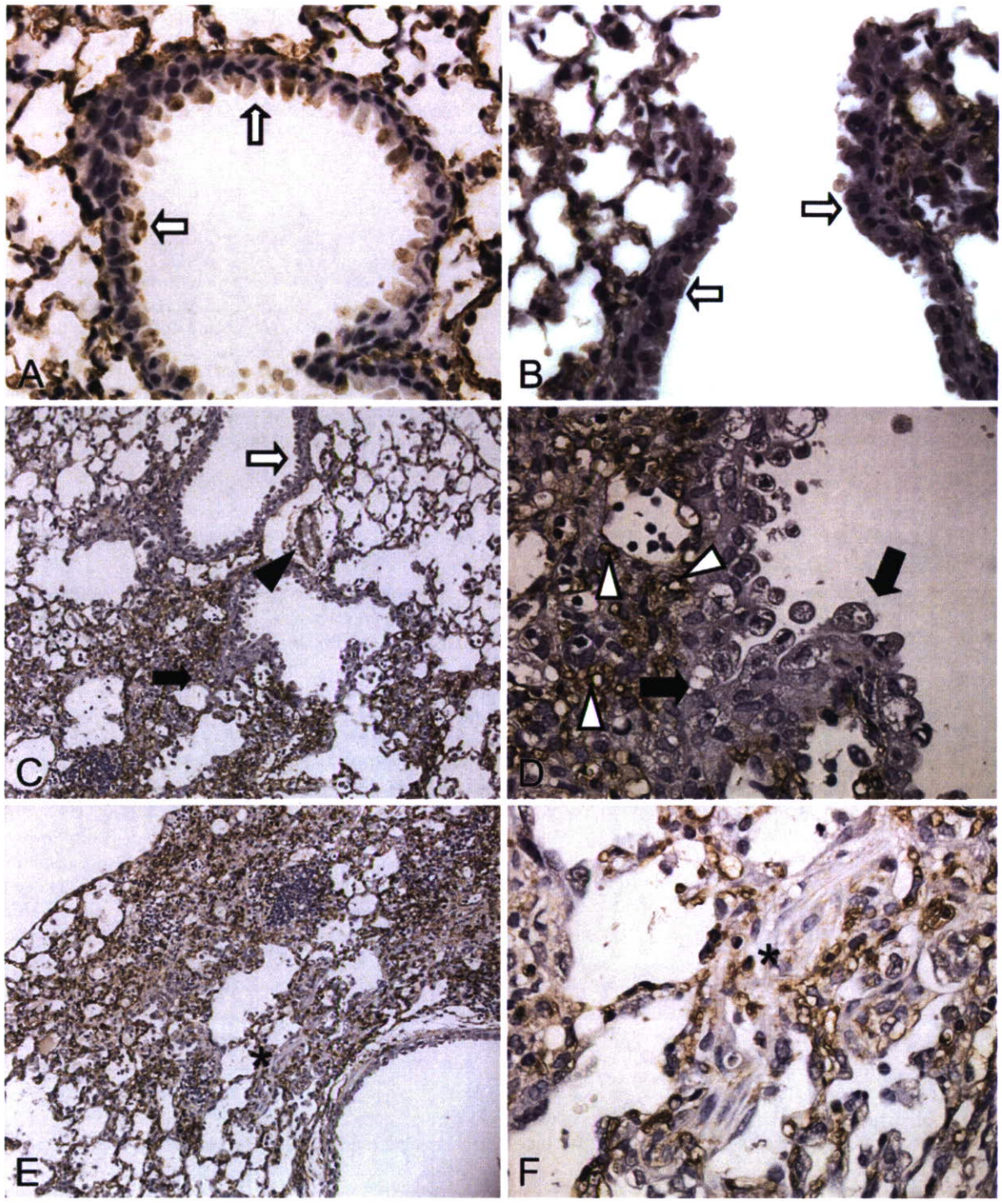


**Figure 1** Immunohistochemical localization of caveolin-1 in mouse lungs. **(A)** Caveolin-1 at apical side of bronchiolar epithelial cells in untreated lung (white arrow). **(B)** Bronchiolar caveolin-1 (white arrow) is diminished at 7 days after bleomycin treatment. **(C,D)** Caveolin-1 is negative both in bronchiolar epithelial cells (white arrow) and bronchiolization (black arrow) but is positive in vascular endothelial cells (black arrowhead) and capillary endothelial cells (white arrowheads) within fibrotic areas at 14 days. **(E,F)** Caveolin-1 is barely detectable in fibroblastic foci (asterisk).

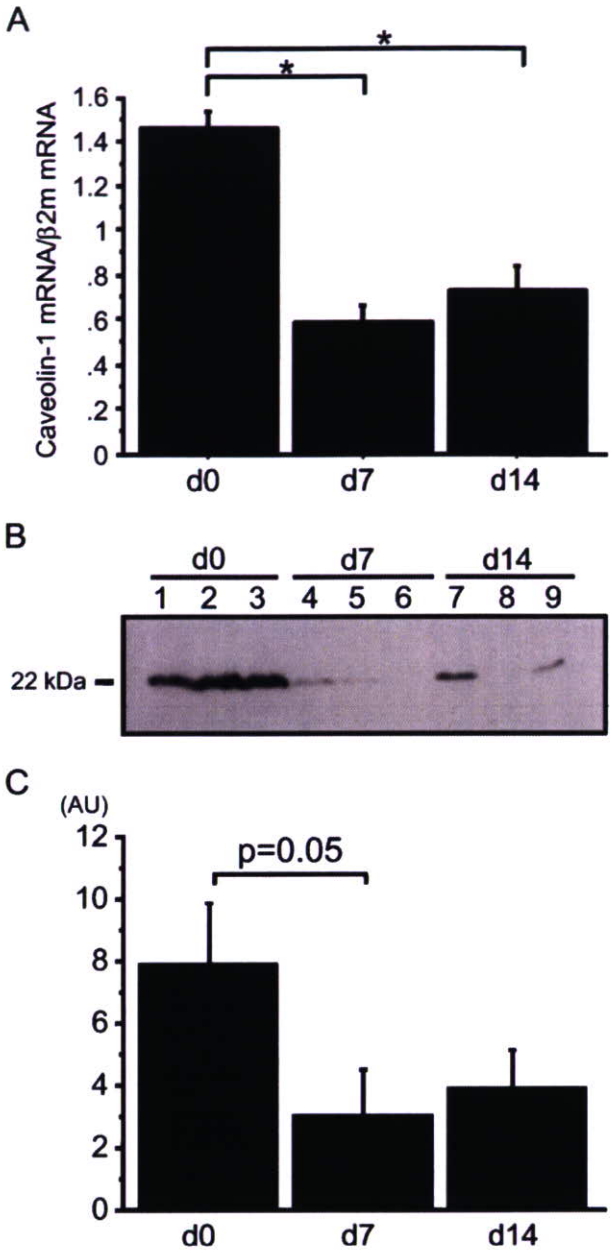


**Figure 2** Expression of caveolin-1 mRNA and protein in whole lungs of mice. d0, untreated control mice; d7, 7 days after bleomycin treatment; d14, 14 days after bleomycin treatment ($n=5$ for each point). **(A)** Caveolin-1 mRNA significantly decreased at 7 and 14 days after bleomycin treatment. **(B)** Caveolin-1 protein in whole lung homogenates detected at 22 kDa by Western blotting. Lanes 1–3, untreated controls (d0); Lanes 4–6, 7 days (d7); Lanes 7–9, 14 days (d14). **(C)** Densitometry shows that caveolin-1 tended to be decreased at 7 days compared with untreated mice ($p=0.05$), but the difference did not reach statistical significance (*$p<0.01$ from untreated mice). β2m, β2-microglobulin; AU, arbitrary units.

### Caveolin-1 mRNA in LCM-retrieved Bronchiolar Epithelial Cells in Mice

We harvested bronchiolar epithelial cells from the lungs using LCM to quantify caveolin-1 mRNA expression in vivo. Figure 3 shows the selective retrieval of terminal bronchiolar epithelium from the mouse lung 7 days after intratracheal bleomycin using LCM. After bleomycin administration, numerous inflammatory cells appeared in the interstitium and additional collagen was deposited around bronchoalveolar junctions (Figure 3A). The tissue retrieved by LCM was confined to terminal bronchiolar epithelium (Figures 3B and 3D), and the tissue remaining after LCM further demonstrated the selectivity of this procedure for removing terminal bronchiolar epithelium (Figure 3C). LCM was not applicable at 14 days after bleomycin exposure. Fibrous deposition at that time surrounded the bronchiolar epithelial cells, thus requiring a more intense or longer laser pulse, either of which enlarged the field and resulted in the retrieval of additional cell types. Caveolin-1 mRNA was detected in bronchiolar epithelial cells retrieved using LCM, and expression levels were significantly decreased at 7 days after bleomycin administration compared with normal lungs ($0.3 \pm 0.1$ vs $0.6 \pm 0.1$, $p<0.01$) (Figure 4).

### Patient Characteristics

Table 1 summarizes the clinical characteristics of patients with IP. Mean interval between onset of symptoms and pathological diagnosis was 13.7 months (UIP, 15.3 months; NSIP, 20.1 months). Two NSIP patients were medicated with oral corticosteroids. None of the patients or normal controls had received any drugs that might cause drug-induced pneumonitis at the time of this study. Vital capacity (% pred) and $DL_{CO}$ (% pred) in IP patients were lower than normal controls. Age, pulmonary function tests, and serum arterial blood gas values did not differ significantly between patients with UIP or NSIP.

### Caveolin-1 mRNA and Protein in Human IPs

We evaluated caveolin-1 mRNA in whole lung homogenates using quantitative RT-PCR. Whole lung caveolin-1 mRNA was significantly decreased in IP patients ($n=12$) including four UIPs and eight NSIPs compared with normal controls ($n=12$) ($0.5 \pm 0.1$ vs $1.1 \pm 0.1$, $p<0.01$) (Figure 5A). Consistent with the mRNA results, Western blotting showed that the protein levels of caveolin-1 in whole lung were significantly decreased in patients with IP ($n=12$) including 4 UIPs and 8 NSIPs, compared with normal controls ($n=12$) ($2.7 \pm 1.0$ AU vs $9.7 \pm 1.2$, $p<0.01$) (Figures 5B and 5C).

### Localization of Caveolin-1 in Human IPs

Caveolin-1 staining was intense in type I epithelial, endothelial, and smooth muscle cells as well as in the api-

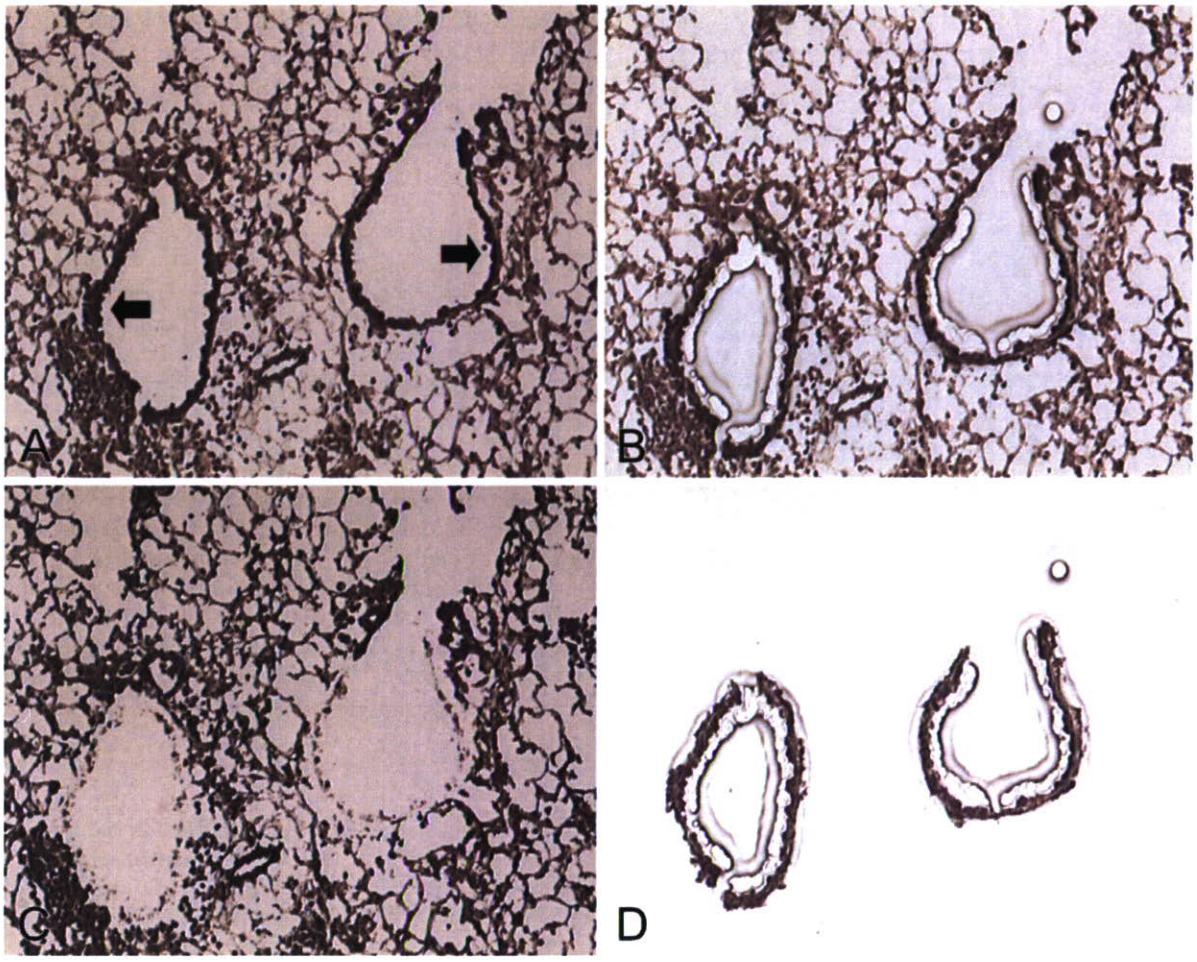


**Figure 3** Laser-capture microdissection (LCM) of bronchiolar epithelial cells from bleomycin-treated lung at 7 days. **(A)** Bronchiolar epithelial cells before capture (arrows). **(B)** Targeted bronchiolar epithelial cells. **(C)** Postdissection photo after removal of bronchiolar epithelial cells. **(D)** LCM-captured bronchiolar epithelial cells on capture disk (Nissl stain).

cal side of bronchiolar epithelial cells of normal lungs (Figure 6A), but not in type II epithelial cells. In lungs of all patients with NSIP, alveolar walls were thickened with edema, fibrosis, inflammatory cell infiltration, and abnormal re-epithelialization. Epithelial cells lining bronchioles within fibrotic areas of IP (Figure 6B), along with areas of abnormal re-epithelialization such as squamous metaplasia (Figure 6C) and non-ciliated (Figure 6D) and ciliated (Figure 6E) bronchiolization were slightly stained for caveolin-1. Ki-67 staining also demonstrated that the rate of proliferation was increased in bronchiolized epithelial cells (see inset in Figure 6D). In addition, caveolin-1 was barely detectable in fibroblastic foci (Figure 6F) as well as in alveolar macrophages and lymphocytes in IPs. In lungs of all patients with UIP, fibrotic zones showed temporal heterogeneity with dense acellular collagen, scattered fibroblastic foci with intervening nearly normal alveoli, honeycombing with complete destruction of the architecture, and abnormal re-epithelialization. Distribution of caveolin-1 in UIP was similar to that of NSIP. Immunoreactive intensity of caveolin-1 was scored for bronchiolar epithelial cells and each type of abnormal re-epithelialization in each patient (Table 2). Caveolin-1 scores did not differ significantly among the types of epithelial cells between UIP and NSIP. Therefore, we combined the UIP and NSIP scores for further analysis. Because there were no differences in staining scores for caveolin-1 between non-ciliated and ciliated bronchiolization ($0.4 \pm 0.2$ vs $0.3 \pm 0.1$, NS), we averaged the staining score for caveolin-1 in bronchiolization for both cell types. The score was significantly lower in bronchiolization, squamous metaplasia, and bronchiolar epithelial cells in fibrotic areas when compared with bronchiolar epithelium in control lungs ($n=7$) ($0.4 \pm 0.1$, $0.1 \pm 0.1$, and $0.4 \pm 0.1$, respectively, vs $1.9 \pm 0.3$,

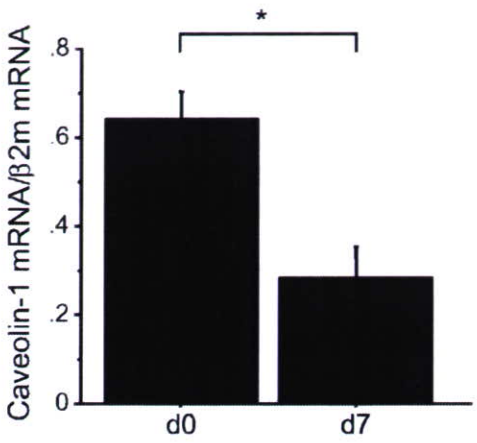


**Figure 4** Expression of caveolin-1 mRNA in mouse bronchiolar epithelial cells retrieved using LCM Caveolin-1 mRNA in bronchiolar epithelial cells retrieved using LCM was significantly decreased compared with these cells in untreated lungs ($n$=5 for each point; *$p$<0.01 compared with untreated lung). β2m, β2-microglobulin; AU, arbitrary units.

$p$<0.01) (Figure 7). Caveolin-1 expression among bronchiolization, squamous metaplasia, and bronchiolar epithelium did not differ significantly in IP patients.

## Discussion

We demonstrated in this study that levels of caveolin-1 decrease in bleomycin-induced lung injury in mice and in human IPs. Furthermore, we found that caveolin-1 is lost in the aberrant re-epithelialization observed in fibrotic regions in mice and humans.

Cell renewal in injured bronchioles and alveoli comprises diversified repair mechanisms, and whether the

**Table 1** Clinical characteristics of IP patients

| | Normal control | IP |
|---|---|---|
| Number of subjects (M/F) | 17 (3/14) | 23 (9/14) |
| Age (years) | 64 ± 2 | 62 ± 2 |
| Cigarette smoking | | |
| Never/former/current | 0/0/0 | 12/4/7 |
| Diagnosis of IP | NA | 12 UIP |
| | | 11 NSIP |
| VC (% pred) | 112 ± 4 | 87 ± 4[a] |
| $FEV_1/FVC$ (%) | 78 ± 1 | 81 ± 1 |
| $DL_{CO}$ (% pred) | 101 ± 4 | 67 ± 6[a] |
| Serum KL-6 (U/ml) | NA | 1165 ± 184 |
| $PaO_2$ (torr) | 81 ± 3 | 80 ± 3 |
| $A\text{-}aDO_2$ (torr) | 16 ± 4 | 19 ± 2 |
| CVD-IP | 0 | 3 SjS |
| | | 1 PM/DM |

[a]$p$<0.01 vs. normal control.
Mean ± SEM. $A\text{-}aDO_2$, alveolar-arterial oxygen difference; CVD-IP, interstitial pneumonia associated with collagen vascular disease; IP, interstitial pneumonia; NA, not available; NSIP, nonspecific interstitial pneumonia; PM/DM, polymyositis/dermatomyositis; SjS, Sjögren's syndrome; UIP, usual interstitial pneumonia.

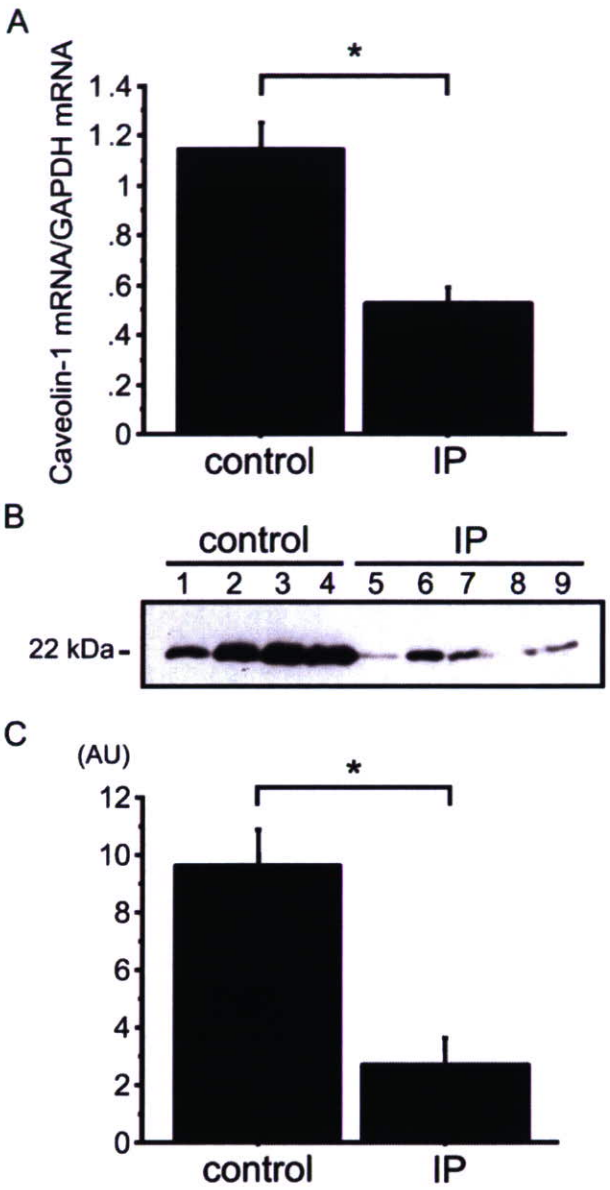


**Figure 5** Expression of caveolin-1 mRNA and protein in human lungs. **(A)** Caveolin-1 mRNA expression in whole lung homogenates is significantly decreased in interstitial pneumonia (IP) patients ($n$=12) compared with control lungs ($n$=12). **(B)** Western blotting shows representative caveolin-1 protein in whole lung homogenates at 22 kDa. Lanes 1–4, control lungs; Lanes 5–9, IP lungs. **(C)** Densitometry shows significantly decreased caveolin-1 in IP ($n$=12) compared with control lungs ($n$=12) (*$p$<0.01 compared with control lungs). GAPDH, glyceraldehyde-3-phosphatase-dehydrogenase; AU, arbitrary units.

appearance of abnormal epithelial cells protects against or promotes fibrosis is uncertain (Portnoy and Mason 2004). We previously reported that gelatinase B [matrix metalloproteinase (MMP)-9] is induced in bronchiolar epithelial cells and in bronchiolization in bleomycin-

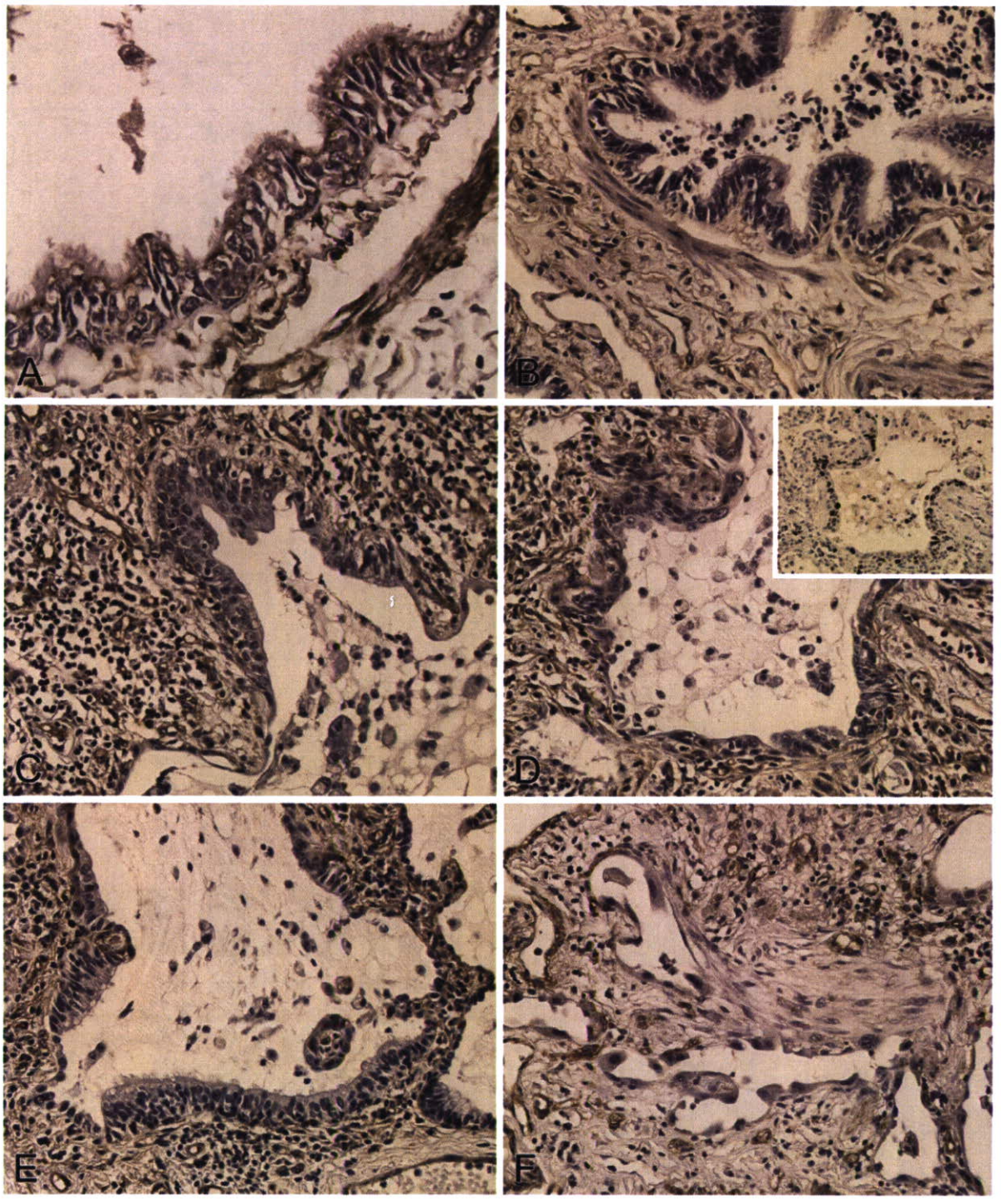


**Figure 6** Immunohistochemical localization of caveolin-1 in human lungs. (**A**) Bronchiolar epithelium in control lung. (**B**) Bronchiolar epithelium in fibrotic area. (**C**) Squamous metaplasia. (**D**) Non-ciliated bronchiolization (Inset; Ki-67 staining). (**E**) Ciliated bronchiolization. (**F**) Fibroblastic foci. (**A**) Control lung. (**B–F**) Nonspecific IP.

**Table 2** Immunohistochemical staining scores for caveolin-1 in bronchiolar epithelium and re-epithelialization in IP patients

| Case no. | Disease | Bronchiolar epithelium in fibrotic area | Squamous metaplasia | Bronchiolization: Non-ciliated | Bronchiolization: Ciliated |
|---|---|---|---|---|---|
| 1 | UIP | 0 | 0 | 0 | 0 |
| 2 | UIP | 0 | 0 | 0 | 0 |
| 3 | UIP | 0 | 0 | 0 | 0 |
| 4 | UIP | 0 | 0 | 0 | 0 |
| 5 | UIP | 1 | 0 | 0 | 0 |
| 6 | UIP | 0 | 0 | 0 | 0 |
| 7 | UIP | 0 | 0 | 0 | 0 |
| 8 | UIP | 1 | 0 | 0 | 0 |
| 9 | UIP | 1 | 2 | 2 | 1 |
| 10 | UIP | 2 | 2 | 2 | 2 |
| 11 | UIP | 0 | 0 | 0 | 1 |
| 12 | UIP | 2 | 1 | 2 | 2 |
| Mean | | 0.4 ± 0.2 | 0.4 ± 0.2 | 0.5 ± 0.3 | 0.5 ± 0.2 |
| 13 | NSIP | 0 | 0 | 0 | 0 |
| 14 | NSIP | 0 | 0 | 1 | 0 |
| 15 | NSIP | 1 | 0 | 1 | 0 |
| 16 | NSIP | 1 | 0 | 0 | 0 |
| 17 | NSIP | 0 | 0 | 0 | 0 |
| 18 | NSIP | 1 | 0 | 0 | 0 |
| 19 | NSIP | 1 | 0 | 1 | 1 |
| 20 | NSIP | 0 | 0 | 0 | 0 |
| 21 | NSIP | 0 | 0 | 0 | 0 |
| 22 | NSIP | 2 | 2 | 0 | 1 |
| 23 | NSIP | 0 | 0 | 0 | 0 |
| Mean | | 0.6 ± 0.2 | 0.2 ± 0.2 | 0.3 ± 0.1 | 0.2 ± 0.1 |

IP, interstitial pneumonia; UIP, usual interstitial pneumonia; NSIP, nonspecific interstitial pneumonia.

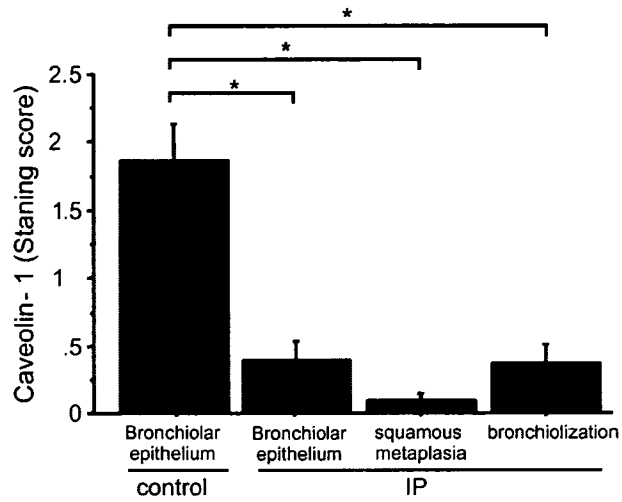


**Figure 7** Immunohistochemical staining scores for caveolin-1. Scores for caveolin-1 in bronchiolar epithelium or each type of re-epithelialization is significantly lower in IP lungs ($n$=23) compared with bronchiolar epithelium in control lungs ($n$=7) (*$p$<0.01).

induced lung fibrosis, and that a gelatinase B deficiency results in defects in alveolar bronchiolization (Betsuyaku et al. 2000). We also reported that expression of the extracellular matrix metalloproteinase inducer (EMMPRIN) increases in bronchiolization in mouse (Betsuyaku et al. 2003a) and in human IP (Odajima et al. 2006). These data imply that EMMPRIN affects re-epithelialization via its capacity to induce MMP expression, leading to bronchiolar epithelial cell migration and proliferation. Excessive caveolin-1 is known to negatively regulate glycosylation and cell surface clustering of EMMPRIN (Tang et al. 2004; Tang and Hemler 2004), which might consequently impair MMP induction. Thus, we speculate that loss of caveolin-1 in bronchiolar epithelial cells might contrarily facilitate glycosylation and self-aggregation of EMMPRIN, leading to excessive MMP induction in those cells in lung fibrosis.

The role of caveolin-1 in airway epithelium has been ignored, partly because of inconsistent identification; caveolin-1 has been detected in bronchiolar epithelial cells by immunohistochemistry in some studies (Kasper et al. 1998; Kato et al. 2004), but not in others (Kogo et al. 2004; Hnasko and Ben-Jonathan 2005; Krasteva et al. 2006). Although these discrepancies have not been explained, the present study demonstrated the steady-state expression of caveolin-1 in bronchiolar epithelial cells at both mRNA and protein levels.

Fibroblastic foci did not express caveolin-1 in the fibrotic lungs of mice and humans in this study, which agrees with the recent finding that fibroblasts harvested from IPF lungs express less caveolin-1 than those from normal lungs (Wang et al. 2006). They also showed that caveolin-1 could suppress transforming growth factor β1-induced extracellular matrix production in cultured fibroblasts. The loss of caveolin-1 in either epithelial or stromal cells independently contributes to the development of mammary hyperplasia and mammary cell transformation (Williams et al. 2006). Together the decrease of caveolin-1 at mRNA and protein levels in whole lung homogenate was probably due to the loss of caveolin-1 in bronchiolization and in fibroblasts as well as in type I epithelial cells (Kasper et al. 1998; Koslowski et al. 2004). The differences at protein levels were detectable in the human specimens but were not statistically significant in the mouse model. Mouse samples are whole lung homogenates in which the fibrosis is sparsely distributed, whereas the human tissue specimens are specifically driven from fibrotic regions. Thus, the decrease of caveolin-1 limited in fibrotic areas might be masked in mouse lung homogenates.

Caveolin-1 suppresses the proliferation and migration of various types of cancer cells in vitro and in vivo (Cohen et al. 2004; Torres et al. 2006). The scaffolding domain of caveolin-1 is a module that inhibits the growth stimulatory activity of several signaling molecules such as tyrosine and serine/threonine kinases, including epidermal growth factor receptor (Couet et al. 1997), mitogen-activated protein kinase, and some of their downstream components (Razani et al. 2002).

Caveolin-1 also interacts with and inactivates some factors in the prosurvival phosphatidylinositol 3-kinase/Akt pathway and platelet-derived growth factor receptor (Liu et al. 1996). It was reported that these signaling molecules are upregulated and associated with lung fibrosis in murine epithelial cells exposed to asbestos (Ramos-Nino et al. 2003). Together the loss of caveolin-1 in bronchiolar epithelial cells in lung fibrosis might progress bronchiolization via the signal transduction of these molecules.

In tumor cells, downregulation of caveolin-1 leads to the loss of E-cadherin, increases transcriptional activity of β-catenin, causes epithelial-to-mesenchymal transition (EMT), and enhances tumor invasion (Lu et al. 2003). In lung fibrosis, β-catenin is reportedly accumulated in nuclei of bronchiolar epithelial cells as well as in regenerated epithelial cells (Chilosi et al. 2003). We then speculate that the downregulation of bronchiolar caveolin-1 might be associated with β-catenin activation, leading to aberrant re-epithelialization and/or EMT in lung fibrosis.

In summary, we demonstrated a significant decrease of caveolin-1 expression, especially in bronchiolar epithelium and in abnormal re-epithelialization in fibrotic lungs.

### Acknowledgments

We thank Ms. Yoko Suzuki for technical assistance with laser-capture microdissection.

## Literature Cited

American Thoracic Society/European Respiratory Society (2002) International multidisciplinary consensus classification of the idiopathic interstitial pneumonias. Am J Respir Crit Care Med 165: 277–304

Barth K, Bläsche R, Kasper M (2006) Lack of evidence for caveolin-1 and CD147 interaction before and after bleomycin-induced lung injury. Histochem Cell Biol 126:563–573

Betsuyaku T, Fukuda Y, Parks WC, Shipley JM, Senior RM (2000) Gelatinase B is required for alveolar bronchiolization after intratracheal bleomycin. Am J Pathol 157:525–535

Betsuyaku T, Griffin GL, Watson MA, Senior RM (2001) Laser capture microdissection and real-time reverse transcriptase/polymerase chain reaction of bronchiolar epithelium after bleomycin. Am J Respir Cell Mol Biol 25:278–284

Betsuyaku T, Kadomatsu K, Griffin GL, Muramatsu T, Senior RM (2003a) Increased basigin in bleomycin-induced lung injury. Am J Respir Cell Mol Biol 28:600–606

Betsuyaku T, Senior RM (2004) Laser capture microdissection and mRNA characterization of mouse airway epithelium: methodological considerations. Micron 35:229–234

Betsuyaku T, Tanino M, Nagai K, Nasuhara Y, Nishimura M, Senior RM (2003b) Extracellular matrix metalloproteinase inducer is increased in smokers' bronchoalveolar lavage fluid. Am J Respir Crit Care Med 168:222–227

Chilosi M, Poletti V, Zamo A, Lestani M, Montagna L, Piccoli P, Pedron S, et al. (2003) Aberrant Wnt/β-catenin pathway activation in idiopathic pulmonary fibrosis. Am J Pathol 162:1495–1502

Cohen AW, Hnasko R, Schubert W, Lisanti MP (2004) Role of caveolae and caveolins in health and disease. Physiol Rev 84: 1341–1379

Couet J, Sargiacomo M, Lisanti MP (1997) Interaction of a receptor tyrosine kinase, EGF-R, with caveolins. Caveolin binding negatively regulates tyrosine and serine/threonine kinase activities. J Biol Chem 272:30429–30438

de Boer WI, Sont JK, van Schadewijk A, Stolk J, van Krieken JH, Hiemstraet PS (2000) Monocyte chemoattractant protein 1, interleukin 8, and chronic airways inflammation in COPD. J Pathol 190:619–626

Drab M, Verkade P, Elger M, Kasper M, Lohn M, Lauterbach B, Menne J, et al. (2001) Loss of caveolae, vascular dysfunction and pulmonary defects in caveolin-1 gene-disrupted mice. Science 293: 2449–2452

Engelman JA, Wykoff CC, Yasuhara S, Song KS, Okamoto T, Lisanti MP (1997) Recombinant expression of caveolin-1 in oncogenically transformed cells abrogates anchorage-independent growth. J Biol Chem 272:16374–16381

Fukuda Y, Ferrans VJ, Schoenberger CI, Rennard SI, Crystal RG (1985) Patterns of pulmonary structural remodeling after experimental paraquat toxicity. The morphogenesis of intraalveolar fibrosis. Am J Pathol 118:452–475

Galbiati F, Volonte D, Engelman JA, Watanabe G, Burk R, Pestell RG, Lisanti MP (1998) Targeted downregulation of caveolin-1 is sufficient to drive cell transformation and hyperactivate the p42/44 MAP kinase cascade. EMBO J 17:6633–6648

Galbiati F, Volonte D, Liu J, Capozza F, Frank PG, Zhu L, Pestell RG, et al. (2001) Caveolin-1 expression negatively regulates cell cycle progression by inducing G(0)/G(1) arrest via a p53/p21(WAF1/Cip1)-dependent mechanism. Mol Biol Cell 12:2229–2244

Glare EM, Divjak M, Bailey MJ, Walters EH (2002) β-Actin and GAPDH housekeeping gene expression in asthmatic airways is variable and not suitable for normalising mRNA levels. Thorax 57:765–770

Hnasko R, Ben-Jonathan N (2005) Developmental regulation of PV-1 in rat lung: association with the nuclear envelope and limited colocalization with Cav-1. Am J Physiol Lung Cell Mol Physiol 288:L275–284

Kasper M, Reimann T, Hempel U, Wenzel KW, Bierhaus A, Schuh D, Dimmer V, et al. (1998) Loss of caveolin expression in type I pneumocytes as an indicator of subcellular alterations during lung fibrogenesis. Histochem Cell Biol 109:41–48

Kato T, Miyamoto M, Kato K, Cho Y, Itoh T, Morikawa T, Okushiba S, et al. (2004) Difference of caveolin-1 expression pattern in human lung neoplastic tissue. Atypical adenomatous hyperplasia, adenocarcinoma and squamous cell carcinoma. Cancer Lett 214:121–128

Kogo H, Aiba T, Fujimoto T (2004) Cell type-specific occurrence of caveolin-1α and -1β in the lung caused by expression of distinct mRNAs. J Biol Chem 279:25574–25581

Koslowski R, Barth K, Augstein A, Tschernig T, Bargsten G, Aufderheide M, Kasper M (2004) A new rat type I-like alveolar epithelial cell line R3/1: bleomycin effects on caveolin expression. Histochem Cell Biol 121:509–519

Krasteva G, Pfeil U, Drab M, Kummer W, Konig P (2006) Caveolin-1 and -2 in airway epithelium: expression and in situ association as detected by FRET-CLSM. Respir Res 7:108

Liu P, Rudick M, Anderson RG (2002) Multiple functions of caveolin-1. J Biol Chem 277:41295–41298

Liu P, Ying Y, Ko YG, Anderson RGW (1996) Localization of the PDGF stimulated phosphorylation cascade to caveolae. J Biol Chem 271:10299–10303

Lu Z, Ghosh S, Wang Z, Hunter T (2003) Downregulation of caveolin-1 function by EGF leads to the loss of E-cadherin, increased transcriptional activity of β-catenin, and enhanced tumor cell invasion. Cancer Cell 4:499–515

Nettesheim P, Szakal AK (1972) Morphogenesis of alveolar bronchiolization. Lab Invest 26:210–219

Odajima N, Betsuyaku T, Nasuhara Y, Itoh T, Fukuda Y, Senior RM, Nishimura M (2006) Extracellular matrix metalloproteinase inducer in interstitial pneumonias. Hum Pathol 37:1058–1065

Portnoy J, Mason RJ (2004) Role of alveolar type II epithelial cells in pulmonary fibrosis. In Lynch JP III, ed. Idiopathic Pulmonary Fibrosis. New York, Marcel Dekker, 573–608

Ramos-Nino ME, Heintz N, Scapoli L, Martinelli M, Land S, Nowak N, Haegens A, et al. (2003) Idiopathic pulmonary fibrosis. Gene profiling and kinase screening in asbestos-exposed epithelial cells and lungs. Am J Respir Cell Mol Biol 29:S51–58

Razani B, Woodman SE, Lisanti MP (2002) Caveolae: from cell biology to animal physiology. Pharmacol Rev 54:431–467

Sato E, Koyama S, Masubuchi T, Takamizawa A, Kubo K, Nagai S, Izumi T (1999) Bleomycin stimulates lung epithelial cells to release neutrophil and monocyte chemotactic activities. Am J Physiol Lung Cell Mol Physiol 276:L941–950

Selman M, King TE Jr, Pardo A (2001) Idiopathic pulmonary fibrosis: prevailing and evolving hypotheses about its pathogenesis and implications for therapy. Ann Intern Med 134:136–151

Simon RH, Paine R (1995) Participation of pulmonary alveolar epithelial cells in lung inflammation. J Lab Clin Med 126:108–118

Tang W, Chang SB, Hemler ME (2004) Links between CD147 function, glycosylation, and caveolin-1. Mol Biol Cell 15:4043–4050

Tang W, Hemler ME (2004) Caveolin-1 regulates matrix metalloproteinases-1 induction and CD147/EMMPRIN cell surface clustering. J Biol Chem 279:11112–11118

Thrall RS, Scalise PJ (1995) Bleomycin. In Phan SH, ed. Pulmonary Fibrosis. New York, Marcel Dekker, 231–292

Torres VA, Tapia JC, Rodríguez DA, Párraga M, Lisboa P, Montoya M, Leyton L, et al. (2006) Caveolin-1 controls cell proliferation and cell death by suppressing expression of the inhibitor of apoptosis protein surviving. J Cell Sci 119:1812–1823

Volonte D, Zhang K, Lisanti MP, Galbiati F (2002) Expression of caveolin-1 induces premature cellular senescence in primary cultures of murine fibroblasts. Mol Biol Cell 13:2502–2517

Wang XM, Zhang Y, Kim HP, Zhou Z, Feghali-Bostwick CA, Liu F, Ifedigbo E, et al. (2006) Caveolin-1: a critical regulator of lung fibrosis in idiopathic pulmonary fibrosis. J Exp Med 203:2895–2906

Williams TM, Lisanti MP (2005) Caveolin-1 in oncogenic transformation, cancer, and metastasis. Am J Physiol Cell Physiol 288: C494–506

Williams TM, Sotgia F, Lee H, Hassan G, Vizio DD, Bonuccelli G, Capozza F, et al. (2006) Stromal and epithelial caveolin-1 both confer a protective effect against mammary hyperplasia and tumorigenesis. Caveolin-1 antagonizes cyclin D1 function in mammary epithelial cells. Am J Pathol 169:1784–1801

Yokoyama A, Kohno N, Hamada H, Sakatani M, Ueda E, Kondo K, Hirasawa Y, et al. (1998) Circulating KL-6 predicts the outcome of rapidly progressive idiopathic pulmonary fibrosis. Am J Respir Crit Care Med 158:1680–1684

The Journal of Histochemistry & Cytochemistry


Connective Tissue Research
Publication details, including instructions for authors and subscription information:
http://www.informaworld.com/smpp/title~content=t713617769

# Differentiation of Tracheal Basal Cells to Ciliated Cells and Tissue Reconstruction on the Synthesized Basement Membrane Substratum **In Vitro**

Takeshi Hosokawa [a]; Tomoko Betsuyaku [a]; Masaharu Nishimura [a]; Akiko Furuyama [b]; Kazuko Katagiri [c]; Katsumi Mochitate [c]
[a] First Department of Medicine, Hokkaido University School of Medicine, Sapporo, Japan
[b] Research Center for Environmental Risk, National Institute for Environmental Studies, Tsukuba, Japan
[c] Environmental Health Science Division, National Institute for Environmental Studies, Tsukuba, Japan

Online Publication Date: 01 January 2007
To cite this Article: Hosokawa, Takeshi, Betsuyaku, Tomoko, Nishimura, Masaharu, Furuyama, Akiko, Katagiri, Kazuko and Mochitate, Katsumi (2007) 'Differentiation of Tracheal Basal Cells to Ciliated Cells and Tissue Reconstruction on the Synthesized Basement Membrane Substratum **In Vitro**', Connective Tissue Research, 48:1, 9 - 18
To link to this article: DOI: 10.1080/03008200601017488
URL: http://dx.doi.org/10.1080/03008200601017488

*Connective Tissue Research*, 48:9–18, 2007

ISSN: 0300-8207 print / 1521-0456 online
DOI: 10.1080/03008200601017488

informa
healthcare

# Differentiation of Tracheal Basal Cells to Ciliated Cells and Tissue Reconstruction on the Synthesized Basement Membrane Substratum *In Vitro*

**Takeshi Hosokawa, Tomoko Betsuyaku, and Masaharu Nishimura**
*First Department of Medicine, Hokkaido University School of Medicine, Sapporo, Japan*

**Akiko Furuyama**
*Research Center for Environmental Risk, National Institute for Environmental Studies, Tsukuba, Japan*

**Kazuko Katagiri and Katsumi Mochitate**
*Environmental Health Science Division, National Institute for Environmental Studies, Tsukuba, Japan*

**Although lung epithelial cells directly attach to the basement membrane underneath *in vivo*, harvested epithelial cells are typically cultured on type I collagen gel (Col I-gel) *in vitro*. Recently we developed new culture substratum, designated as "synthesized Basement Membrane" (sBM), that has bared lamina densa on fibrillar collagen. To validate the usefulness of sBM substratum in airway tissue reconstitution *in vitro*, we cultured rat tracheal epithelial cells on sBM substratum and Col I-gel. When starting the air-liquid interface culture, most of the epithelial cells were squamous and positive for the basal cell marker cytokeratin 14 (CK14). After 14 days on sBM substratum, CK14-positive cells differentiated not only to Clara and mucous cells, but also to ciliated cells. Those differentiated cells formed pseudostratified-like epithelium and the remaining CK14-positive cells were polarized to the basal side. However, on Col I-gel, the CK14-positive cells were still squamous and not polarized, and ciliated cells did not appear. In conclusion, we established a new culture model on sBM substratum in which basal cells could differentiate to ciliated cells. The application of sBM substratum is useful in the study of the airway epithelial cell differentiation *in vitro*.**

**Keywords** Air-Liquid Interface, Airway Epithelial Cells, Basal Cell, Basement Membrane, Cell Differentiation, Extracellular Matrix, Lamina Densa, Laminin, Type IV Collagen

Received 21 April 2006; revised 12 September 2006; accepted 15 September 2006.

This research was supported by the NIES Grant-in-Aid Program for Young Scientists.

Address correspondence to Takeshi Hosokawa, MD, First Department of Medicine, Hokkaido University School of Medicine, N-15, W-7, Kita-ku, Sapporo 060-8638, Japan. E-mail: thoso@med.hokudai.ac.jp

## INTRODUCTION

To investigate the intricate mechanism of the repair process in impaired epithelial tissue, various cell culture models have been developed: air-liquid interface (ALI) culture [1], a defined culture medium containing retinoic acid [2, 3], and type I collagen gel (Col I-gel) substratum [4, 5]. Primary airway epithelial cells isolated by proteolytic treatment of the trachea are used in most culture models [6–8]. The ALI culture and the defined culture medium have considerable advantages for a simplified culture model. ALI culture and retinoic acid have been proven to be not only inhibitors of a squamous metaplastic phenotype, but also powerful inducers of differentiation to ciliated cells [3, 9]. However, the usage of primary airway epithelial cells has disadvantages. The cell suspension is a mixture of differentiated cells such as ciliated and secretory ones and immature cells such as basal ones. Heterogeneities of the cell population make it more difficult to analyze the cell lineage from basal cells to differentiated cells. Low yields also make the preparation laborious. Instead, immortal cell lines derived from airway epithelium appear to be able to replace the primary cells by the homogeneity of their cell population. However, the high proliferation, uncontrollable even by ALI culture and retinoic acid, is disadvantageous for constructing differentiated airway epithelial tissue *in vitro*. In this study, we use the cells that are subcultured twice.

Col-I gel has been used in respiratory cell cultures as a good substratum for promoting cell proliferation and differentiation. However, epithelial tissues *in vivo* normally stand on the basement membrane but not on type I collagen. The basement membrane has a highly integrated architecture composed of specific extracellular matrices such as laminin, type IV collagen, perlecan of heparan sulfate proteoglycan, and entactin

(nidogen); these macromolecular constituents regulate epithelial differentiation and morphogenesis as well as cell attachment and motility. In addition, the basement membrane works as a reservoir of growth factors and cytokines as well as a mechanical support [10, 11]. Although the deposition of laminin is observed beneath the basal epithelial layer on Col I-gel culture by immunofluorescent microscopy, it is not a thin and continuous line as the lamina densa *in vivo* [12]. Instead of Col I-gel, Goto and colleagues [13] have proposed using human amnion as a basement membrane substratum and reconstructing tracheal epithelial tissue using primary epithelial cells prepared from guinea pigs. However, human amnion is not always an available substratum for cell culture.

In previous studies, we have reported that rat immortalized alveolar type II epithelial cells (SV40-T2 cells) cultured on a fibrillar collagen substratum could form a continuous lamina densa in the presence of Matrigel® as an exogenous source of laminin and entactin [14]. The major basement membrane components described above were integrated into the lamina densa [14, 15]. By removing only SV40-T2 cells from the epithelial tissue without harming the remaining extracellular matrix structure, fibrillar collagen matrix with lamina densa on the surface could be easily prepared. We name this substratum "synthesized basement membrane" (sBM). In this study, we report on this new substratum for reconstructing tracheal epithelialium *in vitro* and evaluate the usefulness of sBM substratum in establishing *in vitro* reconstitution of airway epithelial tissue. Even though we seeded the rat tracheal epithelial (RTE) cells that were proliferated and undifferentiated by subculturing the freshly harvested primary cells, they could differentiate to ciliated cells on the sBM substratum, but not on Col I-gel.

## MATERIALS AND METHODS

### Culture Media and Supplements

The basal medium formula was an equal volume mixture of Dulbecco's modified Eagle's medium (DMEM) (#05915, Nissui Pharmaceutical, Tokyo, Japan) and Ham's F12 medium (#N6760, Sigma, St. Louis, MO, USA) containing 10 mM Hepes (Wako Pure Chemicals, Tokyo, Japan), 38 mM sodium bicarbonate, 100 U/ml penicillin G potassium (Meiji Seika Kaisha, Tokyo, Japan), and 100 $\mu$g/ml streptomycin sulfate (#S6501, Sigma). The complete medium formula was the basal medium supplemented with 10 $\mu$g/ml insulin (#I6634, Sigma), 0.1 $\mu$g/ml hydrocortisone (#H0396, Sigma), 0.1 $\mu$g/ml cholera toxin (#100, List Biological Laboratories, Campbell, CA, USA), 5 $\mu$g/ml transferrin (#T1283, Sigma), 50 $\mu$M phosphoethanolamine (#P0503, Sigma), 80 $\mu$M ethanolamine (#E0135, Sigma), 25 ng/ml epidermal growth factor (#EGF-201, Toyobo, Osaka, Japan), 30 $\mu$g/ml bovine pituitary extract (#P1476, Sigma), 0.5 mg/ml bovine serum albumin (#A8806, Sigma), and fresh 50 nM retinoic acid (#R2625, Sigma).

### Antibodies

Mouse monoclonal antibodies for MUC5AC (Clone 45M1, #MS-145-P), $\beta$-Tubulin IV (Clone ONS1A6, #MU-178-UC), and cytokeratin 14 (CK14) (#MAB3232) were purchased from NeoMarkers (Fremont, CA, USA), BioGenex (San Ramon, CA, USA), and Chemicon (Temecula, CA, USA), respectively. Rabbit polyclonal antibodies raised against Clara cell-specific 26-kD protein (CCSP) (#AB3700) and laminin (#10765) were obtained from Chemicon and Progen Biotechnik (Heidelberg, Germany), respectively. Affinity-purified anti-collagen IV antibody (#23709) was purchased from Polysciences (Warrington, PA, USA). Fluorescein-5-isothiocyanate (FITC)-conjugated goat affinity-purified antibodies to mouse (#55518) and to rabbit (#55664) were obtained from MP Biomedicals (Irvine, CA, USA). Normal mouse IgG (#sc-2025) and normal rabbit IgG (#sc-2027) were purchased from Santa Cruz Biotechnology (Santa Cruz, CA, USA).

### Isolation of Rat Tracheal Epithelial Cells

All animals were treated in accordance with the National Institutes of Health guidelines (Guide for the Care and Use of Laboratory Animals). RTE cells were isolated by enzymatic dissociation as previously described [3, 6]. Briefly, after 8- to 14-week-old male Sprague-Dawley rats (Japan Clea, Tokyo, Japan) were put under anesthesia with an intraperitoneal injection of 50 mg/kg sodium pentobarbital and then killed by exsanguination, the tracheas were removed and filled with 1% Pronase E (#P5147, Sigma) in Ham's F12 medium through a cannula, and then treated overnight at 4°C. The dissociated cells were flushed out with Ham's F12 medium containing 5% fetal bovine serum (FBS) (Hyclone Laboratories, Logan, UT, USA), and collected at 4°C by centrifugation at 500 × g for 10 min. The recovered cells were suspended in Ham's F12 medium containing 0.5 mg/ml DNase I (#104159, Roche Diagnostics, Indianapolis, IN, USA) and 10 mg/ml bovine serum albumin to dissociate cell aggregates. After a 5-min treatment in an ice bath, the cells were spun down for 5 min and suspended in the complete medium containing 3 mg/ml bovine serum albumin.

### Subculture of Primary RTE Cells

The primary RTE cells were subcultured on collagen coat plates in the complete medium. Six-well nontissue culture treated plates (#1146, Becton Dickinson Labware, Franklin Lakes, NJ, USA) were treated with 2.5 ml of 0.1 mg/ml acid-extracted type I collagen from bovine dermis (#IAC-13, Koken, Tokyo, Japan) in 1 mM HCl solution for 15 min. After the solution was removed, the culture plates were air-dried for more than 8 hr. The RTE cells obtained from 2 rats were combined, seeded on a collagen-coated well, and cultured at 37°C in a humidified atmosphere with 5% $CO_2$. On day 1, the nonadherent cells were removed and complete medium was supplied every 2 to 3 days. When the RTE cells reached 80% confluence, they were subcultured, undergoing treatment first

with Dulbecco's phosphate-buffered saline without calcium and magnesium [D-PBS(−)] at 37°C for 5 min and next with 0.25% trypsin-1 mM EDTA (#25200-056, Gibco Laboratories, Grand Island, NY, USA) for 6 min. The reaction of trypsin was stopped with Ham's F12 medium containing 10% FBS, and the cells were collected by centrifugation at 500 × g for 5 min. They were suspended with the complete medium and seeded on collagen coated plates. In this study, we use two types of RTE cells: one was freshly harvested primary RTE cells; a the other was subcultured RTE cells.

### Type I Collagen Gel Substratum

An acid-extracted type I collagen solution at the concentration of 3 mg/ml neutralized in DMEM, pH 7.2 was placed on the polyethylene terephthalate (PET) membrane of a cell culture insert (#3102, Becton Dickinson Labware) and allowed to polymerize at 37°C in $CO_2$ incubator for 1 hr. After polymerization, the Col I-gel substratum was used for the RTE cell culture.

### Synthesized Basement Membrane Substratum

sBM was prepared as previously described [14] (Figure 1). An acid-extracted type I collagen solution at the concentration of 0.45 mg/ml neutralized in DMEM, pH 7.2 was placed on the PET membrane of a cell culture insert, polymerized in $CO_2$ incubator for more than 20 hr, air-dried, and rinsed with D-PBS(−) before use. This substratum is stiffer than the Col I-gel substratum to mimic the dense collagen matrix. We designated this hard substrarum as fibrillar collagen substratum. Matrigel® (#354234, Becton Dickinson Labware) was placed on the bottom of a tissue culture plate (#3502, Becton Dickinson Labware) and allowed to polymerize in a $CO_2$ incubator for 1 hr. Immortalized rat alveolar type II epithelial cells transfected with the SV40-large T antigen gene (SV40-T2 cells, a gift from Dr. A. Clement [16]) ($8.0 \times 10^5$) were seeded on the fibrillar collagen substratum and cultured in DMEM containing 1% fetal bovine serum and 0.2 mM ascorbic acid 2-phosphate. After 14 days of culture, the cells were lysed and removed with D-PBS(−) containing 50 mM $NH_4OH$, 0.1% Triton X-100, and protease inhibitor cocktail (5 μg/ml leupeptin [#L2884, Sigma], 5 μg/ml pepstatin A [#P5318], 1 μg/ml antipain [#A6191], 1 μg/ml chymostatin [#C7268], and 5 μg/ml phosphoramidon [#P7385]). The fibrillar collagen substratum holding synthesized lamina densa on the bared surface was termed sBM substratum.

### Preparation of Other Substratum

For laminin-1 coating, PET membrane of cell culture insert was coated with laminin-1 (#354232, Becton Dickinson Labware) solution at the concentration of 10 μg/cm$^2$ in DMEM and placed at 37°C in $CO_2$ incubator overnight. For type I collagen coating, PET membrane of cell culture insert was coated with acid-extracted type I collagen at the concentration of 10 μg/cm$^2$ in 1 mM HCl solution for 15 min. After the solution was removed, the culture inserts were air-dried for more than 8 hr. Fibrillar collagen substratum is the same substratum used for preparation of sBM substratum. In this study, we used 5 substrata: sBM substratum, Col I-gel substratum, fibrillar collagen substratum, type I collagen coating, and laminin-1 coating.

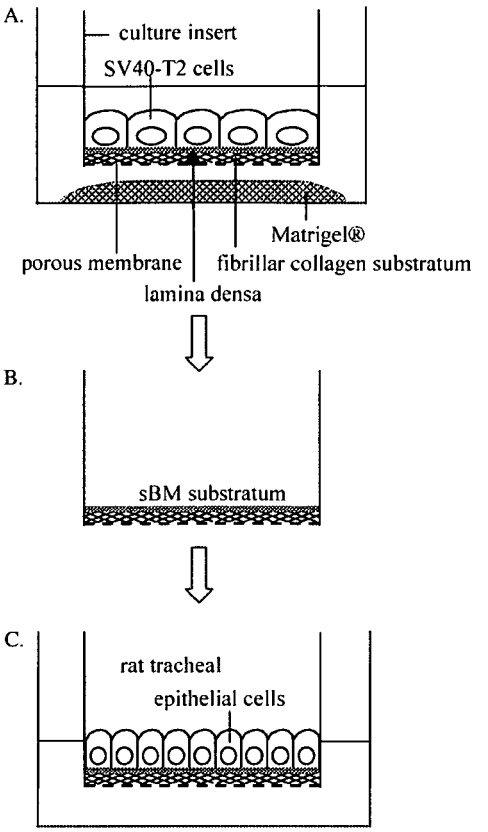


FIG. 1. Preparation of sBM substratum. (A) SV40-T2 cells were cultured on the fibrillar collagen substratum on the porous membrane of a culture insert in the presence of Matrigel®. A lamina densa is formed beneath the SV40-T2 cells. (B) The SV40-T2 cells on the lamina densa were removed and the sBM substratum was prepared. (C) The primary and subcultured rat tracheal epithelial cells were seeded on the sBM substratum and cultured in the air-liquid interface.

### Cell Culture

The primary and subcultured RTE cells were seeded on each substratum at the density of $2.0 \times 10^5$ cells/cm$^2$. Nonadherent RTE cells were removed after 24 hr. The culture medium was changed every other day with 2.5 ml of the complete medium in both compartments. The RTE cells submerged in the medium came to be confluent for 3–7 days and were lifted to the ALI. In the ALI culture, the RTE cells also were placed in a humidified atmosphere with 5% $CO_2$. The apical surface of the cells was

rinsed every other day with Ham's F12 medium and the bottom compartment was filled with only 1.6 ml of the medium.

### Electron Microscopy

All fixatives and dyes for electron microscopy were obtained from TAAB (Berkshire, UK), except for Quetol™ 812 resin (Nissin EM, Tokyo, Japan). Cultured tissues of RTE cells were fixed at 4°C with 4% paraformaldehyde and 2.5% glutaraldehyde in 0.1 M phosphate buffer, pH 7.4, supplemented with 0.2 M sucrose and 0.1% tannic acid, and postfixed with 1% osmium tetraoxide. The tissues were dehydrated through a series of graded ethanol. For scanning electron microscopy, the solvent was replaced with t-butyl alcohol. After the tissues were frozen and lyophilized, they were sputter-coated with a gold/palladium mixture and observed with a JEOL JSM-840 scanning electron microscope. For transmission electron microscopy, the solvent was replaced with n-butyl glycidyl ether and the tissues were embedded in Quetol-812 resin. The embedded tissues were processed to ultrathin sections, stained with lead citrate and uranyl acetate, and examined with a JEOL JEM-2010 microscope.

### Immunofluorescent Microscopy

For immunohistochemical analysis, the cultured tissues were fixed with cold 4% paraformaldehyde in 0.1 M phosphate buffer, pH 7.4, containing 0.2 M sucrose. For vertical observation of the cell layer on a permeable support, tissues were embedded and frozen in Tissue Tek® OTC compound (Miles, Elkhart, IN, USA) and 5-$\mu$m thick transverse sections were cut with a cryostat. The sections were rinsed with 0.1 M phosphate buffer-0.2 M sucrose solution and nonspecific bindings were blocked with normal goat serum (#CL1200, Cedarlane, Ontario, Canada) and bovine serum albumin (#A2058, Sigma). The sections were treated with the primary antibodies in a humidified chamber at room temperature for 30 min. The control sections, which were treated with normal IgG instead of primary antibodies, were run in parallel. FITC-conjugated secondary antibodies were then applied at room temperature for 30 min. The sections were mounted in 4′, 6-diamino-2-phenylindoledihydrochloride (DAPI) in an antifade solution (#S7113, Chemicon) and the resulting fluorescence was observed with a Leica DMRBE microscope.

### Total and Ciliated Cell Counting

To determine the cell densities of RTE cells, the cultured tissues were fixed with cold 4% paraformaldehyde in phosphate buffer-0.2 M sucrose solution and stained the cell nuclei with DAPI. To determine the total cell number, the cell nuclei were counted by immunofluorescent microscopy. The cell numbers in 5 fields of each sample were counted.

The numbers of ciliated cells were counted from the pictures of scanning electron microscopy. The numbers of ciliated cells in 10 fields per sample were counted. The appearance rate of ciliated cells was evaluated as the ratio of the number of ciliated cells to the total number of cells in each culture.

### Western Blot Analysis

Laminin isoform secreted from SV40-T2 cells was detected by Western blot analysis. SV40-T2 cells were cultured on fibrillar collagen substratum in DMEM containing 1% fetal FBS and 0.2 mM ascorbic acid-2-phosphate. After 7 days culture the conditioned medium at the side of basal surface was collected for 3 days from 11th to 14th day and mixed with the protease inhibitors' cocktail of 5 $\mu$g/ml leupeptin, 5 $\mu$g/ml pepstatin A, 1 $\mu$g/ml antipain, 1 $\mu$g/ml chymostatin, and 5 $\mu$g/ml phosphoramidon. The collected medium was further processed to more than 10-fold condensation with microcon centrifugal filter device (Amicon Bioseparations YM-10, Millipore, USA), dissolved in SDS-PAGE sample buffer under reducing condition, and then separated by 5% polyacrylamide gel electrophoresis. The separated proteins were electrophoretically transferred to a polyvinylidene fluoride (PVDF) membrane (Immobilon-P, Millipore) and the laminin isoform was identified with polyclonal antibody for human laminin $\alpha$5 chain (#sc-20145, Santa Cruz) and mouse laminin $\alpha$1-chain (#sc-6017, Santa Cruz). The immunoreactive protein bands were detected by with ECL Plus (Amersham Biosciences, Buckinghamshire, UK) and Polaroid 667. Nonspecific staining was blocked with Block Ace (Dainippon Sumitomo Pharma, Osaka, Japan). Mouse laminin-1 was purchased from Becton Dickinson (#354232). The conditioned medium of the 293 cells endowed with human laminin $\alpha$5-, $\beta$1-, and $\gamma$1-chain genes was the gift from Dr. Karl Tryggvason [17].

### Statistics

Data are expressed as means ± SE. The results were analyzed by one-way analysis of variance for comparison between the two groups. Differences of $p < 0.05$ were considered significant.

## RESULTS

### Preparation of sBM Substratum

The structure of sBM substratum was confirmed by immunofluorescent and electron microscopies as previously described [14]. SV40-T2 cells on fibrillar collagen substratum formed sharp and continuous lamina densa structure beneath the cells (Figure 2A). After SV40-T2 cells were removed from the epithelial tissue, the remaining lamina densa was exposed on the surface of the residual tissue (Figure 2B). The surface of the sBM substratum was a flat and continuous sheet of fine felt-like meshwork (Figure 2C). By immunofluorescent microscopy, a thin and continuous line of laminin and type IV collagen, major basement membrane components, was observed (Figures 2D and 2E). The sBM substratum had the common characteristics of basement membrane structure *in vivo*.

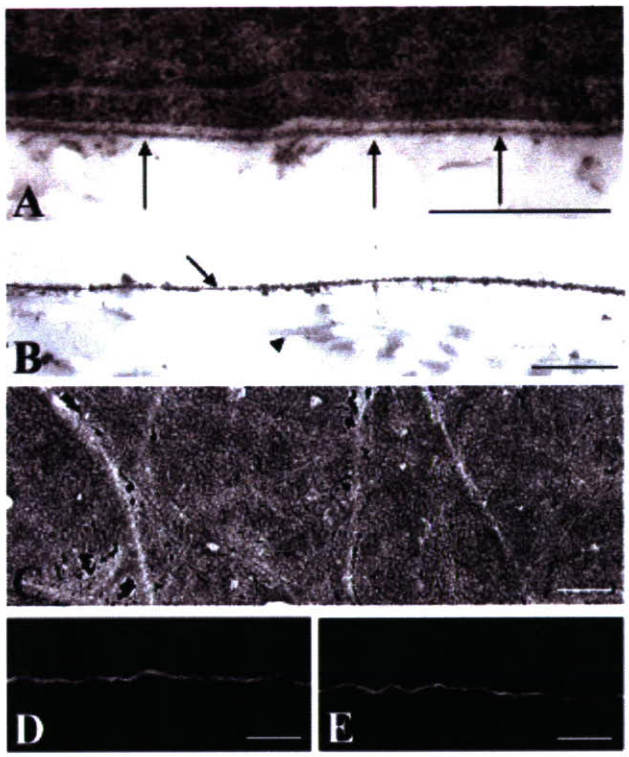


FIG. 2. Electron and immunofluorescent microscopy observations of the sBM substratum formed by SV40-T2 cells *in vitro*. (A) A continuous thin lamina densa (arrows) was formed beneath SV40-T2 cells. (B) SV40-T2 cells were removed and the remaining lamina densa (arrow) was exposed on the surface of the residual tissue. The fibrillar collagen substructure was observed connecting below the lamina densa (arrowhead). (C) The sBM substratum was a flat and continuous sheet and had a fine felt-like meshwork seen by scanning electron microscopy. Observed by immunofluorescent microscopy, laminin (D) and type IV collagen (E) were continuously integrated into a thin layer on the surface of the sBM substratum. Bars = 0.4 $\mu$m (A, B), 1.0 $\mu$m (C), 50 $\mu$m (D, E).

## Differentiation of RTE Cells on Collagen Gel and sBM Substratum

The primary and subcultured RTE cells were seeded on Col I-gel. Some differentiated ciliated cells were observed among the primary RTE cells on day 14 (Figure 3G). Although no ciliated cells were seen among the subcultured RTE cells on Col I-gel (Figure 3H), many ciliated cells were seen among the same cells on the sBM substratum (Figure 3I). The total number of cells on the sBM substratum increased during culture and was significantly higher than that on the Col I-gel on day 14 (Figure 4A). The appearance ratio of ciliated cells to the total number on the sBM substratum on day 14 was significantly higher than that of on the Col I-gel (Figure 4B). By day 14, the cultured epithelium showed pseudostratified-like structure on the sBM substratum, whereas it was still flat on the Col I-gel (Figures 3J, 3K and 3L). The sBM substratum was partially degraded by RTE cells at day 14. These results suggest that the sBM substratum could facilitate the growth and differentiation of RTE cells.

## Polarization of RTE Cells

The number of RTE cells expressing CK14 as a basal cell marker decreased and came to be localized on the basal side in a time-dependent manner on the sBM substratum. In contrast, CK14-positive cells remained dominant and randomly distributed on Col I-gel (Figure 5). The differentiation of subcultured RTE cells to ciliated cells also was confirmed on the sBM substratum, whereas the cells on Col I-gel were negative with immunofluorescent microscopy for $\beta$-tubulin IV (Figures 6A, 6B, and 6C). The CCSP-positive Clara cells (Figures 6D, 6E, and 6F) and the MUC5AC-positive mucous cells (Figures 6G, 6H, and 6I) also were observed on the sBM substratum as the primary and subcultured RTE cells on Col I-gel. These data suggest that the sBM substratum could induce the polarity and the differentiation of the tracheal epithelial tissue, but Col I-gel failed.

### *Differentiation of RTE Cells on Laminin-1*

Laminin-1 is one of the components integrated into the sBM substratum [14]. To investigate the contribution of laminin-1 and type I collagen to the differentiation, the subcultured RTE cells were cultured on a laminin-1 coating, type I collagen coating, and fibrillar collagen substratum (Figure 7). The subcultured RTE cells were not differentiated to ciliated cells on any kind of substratum. These results suggest that laminin-1 or type I collagen alone could not replace sBM substratum.

## Laminin Isoform of SV40-T2 Cells

To identify the laminin isoform of SV40-T2 cells cultured on fibrillar collagen substratum, the condition medium from 11–14 day culture was collected, more than 10-fold condensed, Western blotted, and detected by chemiluminescence with ECL Plus (Figure 8). The protein band of MW 350k was immunoreactive to the antilaminin $\alpha$5-chain polyclonal antibody raised for human H-160 peptide. The positive control of human laminin-10 also was detected in the condition medium of laminin-10-endowed 293 cells. Mouse laminin-1 and FBS were negative. As laminin $\beta$1- and $\gamma$1-chains also were detected in the conditioned medium (data not shown), rat SV40-T2 cells secreted at least laminin-10 isoform. Comparing with laminin $\alpha$5-chain, a trace of protein band was reactive to anti-$\alpha$1-chain polyclonal antibody raised for mouse M-20 peptide only by ECL advance (data not shown).

## DISCUSSION

A primary culture model of airway epithelial cells from a variety of species including rat has been developed for studies of airway physiology in health and disease [3, 6–8, 13, 18–21]. The airway epithelial tissue and surrounding interstitium are complicated in their structure and function,

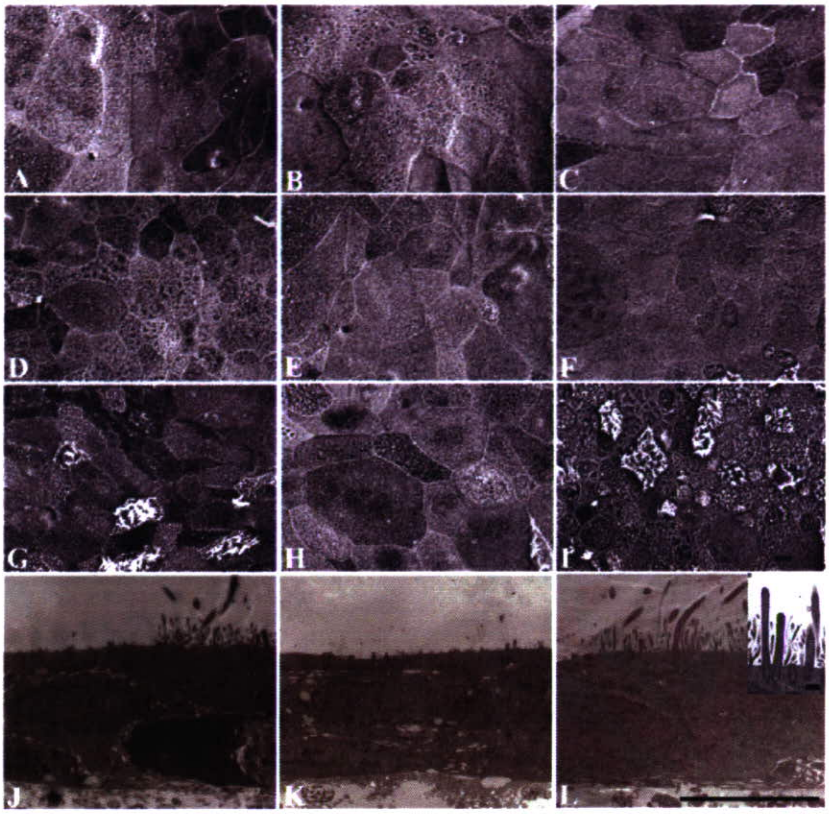


FIG. 3. Scanning electron microscopy observations of cultured epithelial tissue. The primary (A, D, G, J) and subcultured (B, E, H, K) rat tracheal epithelial cells were cultured on Col I-gel. The subcultured cells also were cultured on the sBM substratum (C, F, I, L). The first (A, B, C), the second (D, E, F), and the third (G, H, I) rows are the cultures at days 0, 7, and 14, respectively. The bottom row (J, K, L) is the transmission electron microscopy observation at day 14. The picture of inset (L) is a high magnification of ciliated cell. Bars = 5 $\mu$m (inset 0.5 $\mu$m).

and the epithelial cells constituting the airway surface are associated with each other in the lineage of cell differentiation [22], in which basement membrane beneath the epithelial cells plays crucial roles. Because it has been difficult to mimic the complicated airway epithelial tissues *in vitro*, two important technical clues have been proposed to simplify the culture model: serum-free medium with growth and differentiation supplements including retinoic acid [2, 3] and ALI culture as an inducer of differentiation [1, 9]. Collagen matrix typically has been used for an airway epithelial cell culture model as a solid growth stimulant [4, 23, 24], ignoring that these cells stand on the basement membrane rather than on the type I collagen substructure *in vivo*.

One of the remaining problems is a source of airway epithelial cells; immortalized cell lines such as BEAS-2B [25] and SPOC-1 [26] are not adequate for reconstructing airway tissue *in vitro* because of their high proliferation as well as less normal differentiation. On the other hand, the primary epithelial cells isolated by protease treatment of dissected trachea or bronchi have other disadvantages: low yield, reduced cell adherence, and heterogeneous cell population. The heterogeneity is especially disadvantageous for investigating cell differentiation.

Primary RTE cells are a mixture of heterogeneous cell population: mainly ciliated and secretory cells and a few basal cells. Each cell type appears to have a different adherence activity on culture substratum and the cell adherence changes depending on the impairment degree by the protease treatment in preparation, so that more than half the population of primary cells fails to adhere [27]. These characteristics of the primary cells have made it complicated to analyze the differentiation of basal cells to secretory and ciliated cells *in vitro*. To solve the problem of the heterogeneous population, we subcultured the primary RTE cells on a type I collagen coating up to the second passage and allowed the cells to proliferate, undifferentiating to a homogeneous population of basal cells. However, the immature basal cells alone failed to differentiate to ciliated cells not only on soft (Col I-gel) and stiff (fibrillar collagen substratum) matrices of type I collagen, but also on a laminin-1 coating even in the ALI culture. The basal cells squamously proliferated and multilayered on them. Once

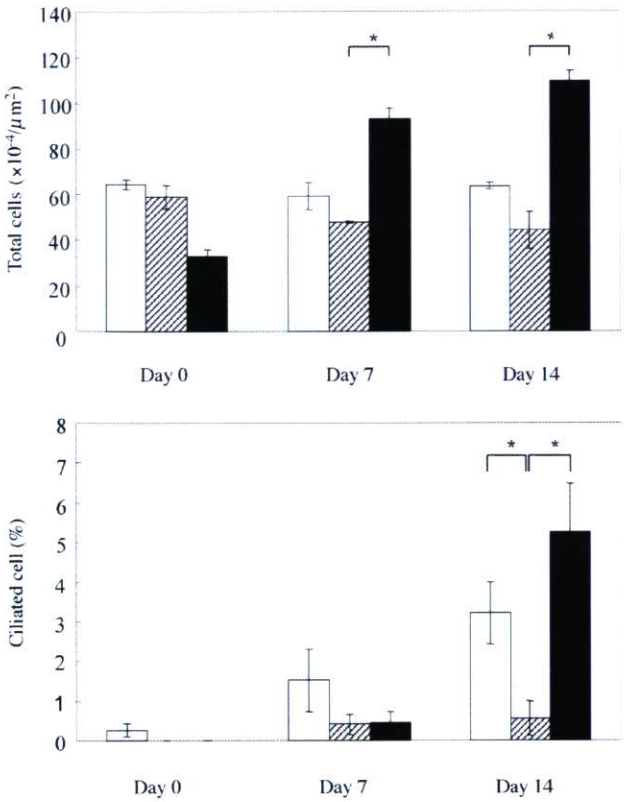


FIG. 4. The primary rat tracheal epithelial cells were cultured on Col I-gel (□). The subcultured rat tracheal epithelial cells were cultured on Col I-gel (▨). The subcultured rat tracheal epithelial cells were cultured on the sBM substratum (■). The total cell number in each culture is seen in upper graph; the appearance rate of ciliated cells in the lower. [Values are expressed as means ± SE; * = significant at $p < .05$.]

the heterogeneous primary cells became an undifferentiated cell population in subculture, those cells appeared to lose the potential of differentiation as long as they were cultured on the traditional substratum.

Recently, we proposed the use of a sBM substratum for epithelial tissue reconstruction [14]. The basement membrane beneath epithelial cells has a highly integrated architecture composed of extracellular matrices including laminin, type IV collagen, heparan sulfate proteoglycan, and entactin (nidogen) [10]. Depending on the biological nature of each component and the relationship between molecular events such as masking and subsequent unmasking by limited proteolysis with matrix metalloproteinases, the basement membrane controls various kinds of cellular behaviors including differentiation [11]. Previously, we reported that alveolar type II epithelial cells immortalized by SV40-large T antigen (SV40-T2 cells) cultured on fibrillar collagen substratum could form the basement membrane beneath the cells with a large amount of exogenous laminin and entactin from Matrigel® [14, 15, 28, 29]. By removing only SV40-T2 cells from the culture tissue without impairing the extracellular matrices, the lamina densa could be prepared. The major basement membrane components were located in the lamina densa. We named this unique substratum sBM. Because not only type I collagen, but also laminin-1 substratum were impotent to realize the potential for differentiation of the immature basal cells, we have shifted to using, sBM substratum for the differentiation of subcultured RTE cells.

The sBM substratum has proved to be powerful for inducing differentiation even after RTE cells were subcultured and undifferentiated to immature cells. The immature RTE cells homogenously expressed basal cell marker CK14 and could differentiate to ciliated cells on the sBM substratum. The differentiation of the subcultured basal cells on the sBM substratum was superior to that of the same cells on type I collagen substratum in the population of ciliated cells, and comparable with those of MUC5AC-positive and CCSP-positive cells. In addition, the CK14-positive cells on the sBM substratum were well polarized in the pseudostratified-like tissue developed from the homogenous subcultured basal cells, while the cells scarcely polarized in the squamously developed tissue on Col I-gel. This polarization of CK14-positive cells is similar to the observation

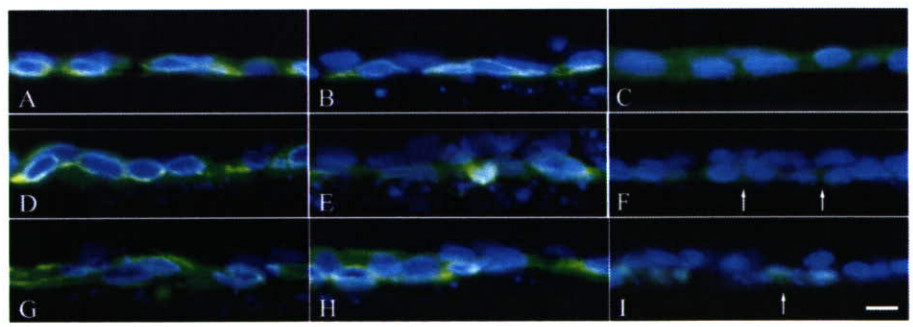


FIG. 5. Immunofluorescent microscopy observations of rat tracheal epithelial cells with anti-CK14 antibody as a basal cell marker. The primary (A, D, G) and subcultured (B, E, H) rat tracheal epithelial cells were cultured on Col I-gel. The subcultured rat tracheal epithelial cells were cultured on sBM substratum (C, F, I). The upper (A, B, C), the middle (D, E, F), and the lower (G, H, I) rows are the cultured epithelial tissues at days 0, 7, and 14, respectively. The basal cell marker CK14 was stained in green (arrows) with FITC and the nuclei were stained blue with DAPI. (Bars = 10 μm.)